The extended Perdew-Burke-Ernzerhof functional with improved accuracy for thermodynamic and electronic properties of molecular systems

Xin Xu[a)]
*State Key Laboratory for Physical Chemistry of Solid Surfaces, Center for Theoretical Chemistry,
Department of Chemistry, Xiamen University, Xiamen 361005, China and Materials and Process Simulation
Center (139-74), California Institute of Technology, Pasadena, California 91125*

William A. Goddard III[b)]
*Materials and Process Simulation Center (139-74), California Institute of Technology,
Pasadena, California 91125*

Density functional theory (DFT) has become the method of choice for many applications of quantum mechanics to the study of the electronic properties of molecules and solids. Despite the enormous progress in improving the functionals, the current generation is inadequate for many important applications. As part of the quest of finding better functionals, we consider in this paper the Perdew-Burke-Ernzerhof (PBE) functional, which we believe to have the best theoretical foundation, but which leads to unacceptable errors in predicting thermochemical data (heats of formation) of molecular systems [mean absolute deviation (MAD)=16.9 kcal/mol against the extended $G2$ data set of 148 molecules]. Much improved thermochemistry is obtained with hybrid DFT methods that include part of the Hartree-Fock exchange [thus B3LYP (Becke's three parameter scheme combining Hartree-Fock exchange, Becke gradient corrected exchange functional and Lee-Yang-Parr correlational functional) with MAD=3.1 kcal/mol and PBE0 (Perdew's hybrid scheme using PBE exchange and correlation functionals) with MAD=4.8 kcal/mol]. However we wish to continue the quest for a pure density-based DFT. Thus we optimized the four free parameters (μ, κ, α, and β) in PBE theory against experimental atomic data and the *van der Waals* interaction properties of Ne_2, leading to the *xPBE extended functional*, which significantly outperforms PBE for thermochemical properties MAD reduced to 8.0 kcal/mol while being competitive or better than PBE for predictions of geometric parameters, ionization potentials, electron affinities, and proton affinities and for the description of van der Waals and hydrogen bond interactions. Thus xPBE significantly enlarges the field of applications available for pure DFT. The functional forms thus obtained for the exchange and correlational functionals may be useful for discovering new improved functionals or formalisms. © *2004 American Institute of Physics.* [DOI: 10.1063/1.1771632]

I. INTRODUCTION

Density functional theory[1] (DFT) has become a valuable alternative to the conventional Hartree-Fock (HF) and post-HF methods[2] for the study of molecular electronic structures. DFT replaces the conventional *ab initio* wave function, which depends on $4N$ variables (three spatial and one spin variable for each of the N electrons), by the electron density, which depends only on the three spatial variables, as a means to reach a solution to the Schrödinger equation in DFT. In principle, DFT takes into full account all many-body effects with computation costs comparable with mean field (Hartree) approximations.[1] Unfortunately, the exact density functional is unknown, making it necessary to develop approximate functionals using theory to help to specify limits and functional forms and comparisons to accurate experiments to determine a limited set of parameters. Therefore, the quest of finding better and better functionals is at the heart of density functional theory.

Many approximations to the exchange-correlation energy have been developed and tested. The simplest approximation is the local density approximation (LDA) based on fitting the exact numerical results from the uniform electron gas (UEG).[3–5] While LDA yields results of good or moderate accuracy for some properties (lattice constants, bulk moduli, equilibrium geometries, and vibrational frequencies) (Ref. 6) the severe overbinding of LDA [mean absolute deviation (MAD)=90.9 kcal/mol for the $G2$ data set of 148 atoms and molecules] makes corrections depending on the density derivatives essential.[7] The generalized gradient approximations (GGAs) use exchange functionals including the first-order gradients[8] and have demonstrated great improvement over LDA for bond energies of molecules, the cohesive energies of solids, and the energy barriers for molecular reactions, but they generally remain inadequate for thermochemistry for molecules.

Several GGA functionals[8–22] have proved useful in applications to molecules and solids, but Perdew, Burke, and Ernzerhof [PBE (Ref. 11)] have developed a simplified GGA that best fulfills many of the physical and mathematical requirements of DFT. In particular, PBE (a) satisfies the Lieb-

---

[a)]Electronic mail: xinxu@xmu.edu.cn
[b)]Electronic mail: wag@wag.caltech.edu

Oxford bound[23] (that is, $E_x[\rho] \geqslant E_{xc}[\rho] \geqslant -1.679 \int d^3 r \rho(r)^{4/3}$); (b) provides the correct linear response of the uniform electron gas with proper uniform scaling;[24] and (c) leads to smooth pseudopotentials.[11]

However, the numerical performance of PBE is unsatisfactory for total atomic energies and thermochemical properties of molecular systems.[12] For example, Handy and co-workers designed a test of 93 chemical systems that DFT methods should satisfy to be recommended for chemistry and concluded PBE does not pass.[25]

The most successful DFT functionals for thermochemistry [e.g., B3LYP (Ref. 26) and PBE (Ref. 21)] include in the exchange energy a component of exact Hartree-Fock exchange (using Kohn-Sham orbitals); however, this comes at considerable computational cost (particularly for infinite systems), which we wish to avoid, and these hybrid methods violate the spirit of DFT that the energy expression depends only on the local density.

We present here an extension of the PBE functional (denoted as xPBE) in which we optimize four parameters (μ, κ, α, and β) in PBE against (a) experimental atomic data and (b) the *van der Waals* interaction properties of Ne_2, (c) but using no other molecular data. We find that the xPBE extended functional significantly outperforms PBE in predicting (i) atomic data (exchange energies, correlation energies, and total energies for atoms from H to Ar) and (ii) thermochemistry (heats of formation for the extended $G2$ set).[27,28] At the same time, xPBE is competitive or of better quality than PBE in the predictions of (1) geometric parameters, ionization potentials, electron affinities, and proton affinities (against the extended $G2$ set) (Refs. 27 and 29), and (2) van der Waals and (3) hydrogen bond interactions, thus greatly enlarging the original field of applications.

II. THEORETICAL BACKGROUND

A. GGA exchange and correlation functional

In the Kohn-Sham formalism for DFT, the total energy is written as

$$E = KE + CE + E_{xc} \tag{1}$$

where KE is the kinetic energy of the Kohn-Sham orbitals, CE is the classical Coulomb interaction energy for the total density constructed from the Kohn-Sham orbitals, and the exchange-correlation functional E_{xc}, includes everything else. The challenge is to describe the E_{xc} term, which, conventionally, is assumed that to be separable,

$$E_{xc} = E_x + E_c. \tag{2}$$

In GGA,[8] the exchange functional is expressed as

$$E_x^{GGA} = \int d^3 r \rho(r) \epsilon_x^{unif}(\rho) F_x(s), \tag{3}$$

where $\rho(r)$ is the total density; $\epsilon_x^{unif} = -3k_F/(4\pi)$ is the Slater exchange energy density in the uniform electron gas approximation,[3,4] $k_F = [3\pi^2 \rho(r)]^{1/3}$ is the local Fermi wave vector, and $F_x(s)$ is the GGA enhancement factor depending on a dimensionless density gradient s, which is defined as $s = |\nabla \rho|/(2k_F \rho)$.

The GGA (Ref. 17) correlation functional is expressed as

$$E_c^{GGA}[\rho^\uparrow \rho^\downarrow] = \int d^3 r \rho(r)[\epsilon_c^{unif}(r_s, \zeta) + H(r_s, \zeta, t)], \tag{4}$$

where r_s is the local Seitz radius defined as $r_s = [(4\pi/3)\rho(r)]^{1/3}$, $\zeta = (\rho^\uparrow - \rho^\downarrow)/\rho$ is the relative spin polarization, and $t = |\nabla \rho|/(2gk_s \rho)$ is another scaled density gradient. Here $g = [(1+\zeta)^{2/3} + (1-\zeta)^{2/3}]/2$ is a spin-scaling factor and $k_s = (4k_F/\pi)^{1/2}$ is the Thomas-Fermi screening wave vector.

Similar to Eq. (3), we may express Eq. (4) as

$$E_c^{GGA} = \int d^3 r \rho(r) \epsilon_c^{unif}(\rho) F_c(r_s, \zeta, t). \tag{5}$$

Thus we define

$$F_c(r_s, \zeta, t) \equiv 1 + \frac{H(r_s, \zeta, t)}{\epsilon_c^{unif}(r_s, \zeta)}. \tag{6}$$

Conventionally, we may define the enhancement factor F_{xc} over local exchange[11]

$$E_{XC}^{GGA} = \int d^3 r \rho(r) \epsilon_x^{unif}(\rho) F_{xc}(r_s, \zeta, s). \tag{7}$$

Thus we have

$$F_{xc}(r_s, \zeta, s) \equiv F_x(s) + \frac{\epsilon_c^{unif}(r_s, \zeta)}{\epsilon_x^{unif}(\rho)} F_c(r_s, \zeta, t). \tag{8}$$

In the well-established Perdew-Wang-91 correlation functional [PW91 (Ref. 17)], H is expanded as

$$H = H_0 + H_1, \tag{9}$$

where

$$H_0 = g^3 \frac{\beta^2}{2\alpha} \ln\left[1 + \frac{2\alpha}{\beta} \frac{t^2 + At^4}{1 + At^2 + A^2 t^4}\right], \tag{10}$$

$$H_1 = \left(\frac{16}{\pi}\right)(3\pi^2)^{1/3}\left[C_c(r_s) - C_c(0) - \frac{3C_X}{7}\right]g^3 t^2$$

$$\times \exp\left[-100g^4 t^2\left(\frac{k_s^2}{k_F^2}\right)\right], \tag{11}$$

with parameters $A = 2\alpha/(\beta(\exp[-2\alpha\epsilon_c^{unif}(r_s, \zeta)/(g^3\beta^2)] - 1))$, $\alpha = 0.09$, $\beta = 0.066\,725$, the Rasolt and Geldart constants C_c (Ref. 30) and the Sham coefficient C_X.[31]

B. The PBE exchange and correlation functional

In PBE, the enhancement factor of the exchange functional takes the form

$$F_x^{PBE}(s) = 1 + \kappa - \frac{\kappa}{\left(1 + \frac{\mu}{\kappa}s^2\right)}, \tag{12}$$

where $\kappa = 0.804$ is set to the maximum value allowed by the local Lieb-Oxford bound[24] on E_{xc} and $\mu = 0.219\,51$ is set to

recover the linear response of the uniform gas such that the effective gradient coefficient for exchange cancels that for correlation.

In the PBE correlation functional, only the first term in the PW91 correlation functional is kept:

$$H^{PBE} = H_0 = g^3 \frac{\beta^2}{2\alpha} \ln\left[1 + \frac{2\alpha}{\beta} \frac{t^2 + At^4}{1 + At^2 + A^2 t^4} \right]. \tag{13}$$

This was derived from three limits,

$$H^{PBE} \rightarrow \beta g^3 t^2 \quad (\text{as } t \rightarrow 0), \tag{14}$$

$$H^{PBE} \rightarrow -\epsilon_C^{unif} \quad (\text{as } t \rightarrow \infty), \tag{15}$$

and

$$E_C^{PBE}[\rho_\gamma^\uparrow, \rho_\gamma^\downarrow] \rightarrow \text{const} \quad (\gamma \rightarrow \infty), \tag{16}$$

where $\rho_\gamma(r) = \gamma^3 \rho(\gamma r)$ is a uniformly scaled density.[24] Note that the last constraint is violated by PW91 because of H_1 term.

In addition PBE uses $\alpha = 0.0716$ instead of $\alpha = 0.09$ used in PW91.

III. THE EXTENDED PBE FUNCTIONAL: xPBE

A. The μ term

Taking a Taylor series expansion of the PBE exchange functional around $s = 0$ leads to

$$F_x^{PBE}(s) = 1 + \mu s^2 - \frac{\mu^2}{\kappa} s^4 + \cdots, \tag{17}$$

PBE chooses $\mu = 0.21951$ based on a theoretical analysis.[11] However, there are alternative theoretical deductions of μ.[31–38] Based on wave-vector analysis, μ was determined as $\frac{10}{81} = 0.12346$ in the slowly varying limit.[31] Very recently, Hirao and co-workers arrived at $\mu = \frac{20}{81} = 0.24692$, and suggested that the previous value of $\frac{10}{81}$ might have been incorrect.[38] μ has also been empirically determined by fitting to certain set of the experimental data. For example, the popular Becke88 functional uses $\mu = 0.27429$.[9] Becke was the first to propose using the exchange functional of Eq. (12), where in B86 the parameters $\mu = 0.23511$ and $\kappa = 0.9672$ were determined by a least squares fit to the Hartree-Fock exchange energies of the 20 atomic systems H through Ar, plus Kr and Xe.[15]

B. The κ term

Perdew, Burke, and Wang[39] compared the PBE enhancement factor of Eq. (12) with various numerical results for $F_x(s)$ as a function of s in the physical range $0 \leq s \leq 3$. They showed that a sharp radial cutoff corresponds well to $\kappa = 0.804$, while a more diffuse cutoff leads to a smaller value of κ. This uncertainty is also reflected in the PBE derivation of Eq. (12), in which κ is set to the maximum value of the local Lieb-Oxford bound.[11] Lacks and Gordon argued that the local Lieb-Oxford bound is not a necessary criterion for an exchange functional.[40] Zhang and Yang [revPBE (Ref. 12)] relaxed this constraint and optimized κ by fitting the exchange-only total atomic energies from He to

TABLE I. The $\{\mu, \kappa, \alpha, \beta\}$ parameters for the functionals in the PBE family. For definitions of the parameters see Eqs. (11) and (12).

	PBE	revPBE	B86PBE	xPBE
κ	0.804	1.245	0.9672	0.91954
μ	0.21951	0.21951	0.23511	0.23214
α	0.0716	0.0716	0.0716	0.197363
β	0.066725	0.066725	0.066725	0.089809

Ar to the exact exchange-only results from the optimized exchange potential method,[41] obtaining $\kappa = 1.245$.[12]

C. The β and α terms

The μ in the PBE exchange functional is correlated with the β in the PBE correlation functional.[11] Any change of μ might require a related change in β to preserve a good LSD (local spin density approximation) description of the exchange-correlation energy in the linear response of the uniform gas. We consider that there is some flexibility for optimizing the α [$\alpha = 0.0716$ in PBE (Ref. 11) and $\alpha = 0.09$ in PW91 (Ref. 17)].

D. Optimization

We will treat the μ and κ parameters in the PBE exchange functional and the α and β parameters in the PBE correlation functional as four parameters to be optimized. To optimize these parameters we will fit data of the following three subsets: (1) the Hartree-Fock limit energies of 18 atoms from H to Ar;[42] (2) the exact total atomic energies from H to Ar;[42] and (3) the binding energy and bond distance of Ne$_2$.[43]

The procedure is

$$\nabla = \sum_{i=1}^{n} \left(\frac{E_i}{E_i^{ref}} - 1 \right)^2 w_i. \tag{18}$$

We minimize the least-square error ∇ in a self-consistent way of solving unrestricted Kohn-Sham orbital equations using aug-cc-pVTZ basis set. Here E_i is the calculated energy and E_i^{ref} is the corresponding reference energy[42,43] in subsets (1)–(3). All energies are in atomic units. The relative weights w_i are adjusted to give a reasonable balance of different contributions. For atomic energies, we use unit weight, except that of H, for which we use a value of 3×10^3. For the binding energy of Ne$_2$, a large weight of 3×10^7 is used. We optimize $\{\mu, \kappa, \alpha, \beta\}$ with i running over all data in three subsets such that $n = 37$ in Eq. (18). While a good fit of the calculated exchange-only total atomic energies against the data in subset (1) leads to suitable μ and κ; a good fit of the calculated exchange-correlation total atomic energies against the data of subset (2) leads to suitable α and β for given μ and κ. Subset (3) provides a constraint on the optimized μ, κ, α, and β for the large gradient/small density limits corresponding to large s and t. We search $\{\mu, \kappa, \alpha, \beta\}$ sequentially to achieve a minimum in the least-square error ∇ for the whole set.

The final results for the four parameters $\{\mu, \kappa, \alpha, \beta\}$ of xPBE listed in Table I where they are compared to the values for PBE, revPBE, and B86PBE. [Note that the notation PBE signifies that the PBE exchange functional is combined with
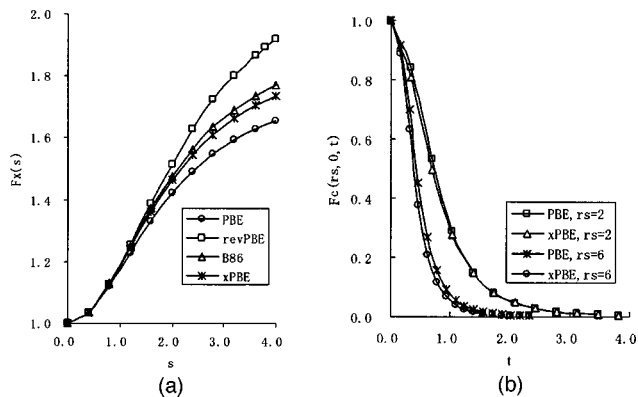
FIG. 1. (a) The enhancement factor $F_x(s)$, Eq. (12), for the exchange functionals in the PBE family. For all curves the $s \to 0$ asymptote is 1.0, recovering the LSD limit. The $s \to \infty$ asymptotes are $1+\kappa=1.804$ (PBE), 2.245 (revPBE), 1.9672 (B86), and 1.919 54 (xPBE). (b) shows the enhancement factor $F_c(r_s, \zeta, t)$, Eq. (6), for the correlation functionals in the PBE family for a spin-unpolarized ($\zeta=0$) case with $r_s=2$ and 6. For all curves the $t \to 0$ asymptote is 1.0, recovering the LSD limit. The $t \to \infty$ asymptote is 0.0, with correlation effects vanishing.

the PBE correlation functional; xPBE indicates our extended PBE exchange functional combined with our extended PBE correlation functional; while revPBE and B86PBE share the same correlation functional with PBE.] We find the follow-

ing: (a) $\alpha=0.197\,363$ is more than twice of the PBE [0.0716 (Ref. 11)] and PW91 [0.09 (Ref. 17)] values, (b) $\beta=0.089\,809$ is 1/3 times larger than PBE [0.066\,725 (Ref. 11)]. (c) $\mu=0.232\,14$ is somewhat larger than that in PBE (0.219\,51), nearly twice the theoretical value [0.123\,46 (Ref. 31)] but quite close to the theoretical value found by Hirao [0.246\,92 (Ref. 38)] and to that proposed in B86 [0.235\,11 (Ref. 15)], (d) $\kappa=0.919\,54$ is in between the value in PBE [0.804 (Ref. 11)] and that in B86 [0.9672 (Ref. 15)].

The final functional forms for $F_x^{\text{xPBE}}(s)$, $F_c^{\text{xPBE}}(r_s, \zeta = 0, t)$ and $F_{\text{xc}}^{\text{xPBE}}(r_s, \zeta = 0, s)$ are shown in Figs. 1, and 2, respectively. Figure 1(a) represents the enhancement factor $F_x(s)$, Eq. (12), for the exchange functionals in the PBE family. The $s \to 0$ asymptote for all curves is 1.0, recovering the LSD limit. The $s \to \infty$ asymptotes are $1+\kappa=1.804$ (PBE), 2.245 (revPBE), 1.9672 (B86), and 1.919\,54 (xPBE) such that the latter three do not support the local interpretation of the global Lieb-Oxford bound.[1,24] Figure 1(b) shows the enhancement factor $F_c(r_s, \zeta, t)$, Eq. (6), for the correlation functionals in the PBE family for a spin-unpolarized ($\zeta=0$) case with $r_s=2$ and 6. The $t \to 0$ asymptote for all curves is 1.0, recovering the LSD limit. The $t \to \infty$ asymptote is 0.0 such that the correlation effects vanish. Figure 2 depicts the enhancement factor $F_{\text{xc}}(r_s, \zeta, s)$, Eq. (8), for the functionals in the PBE family. The $s \to 0$ asymptotes for all curves are

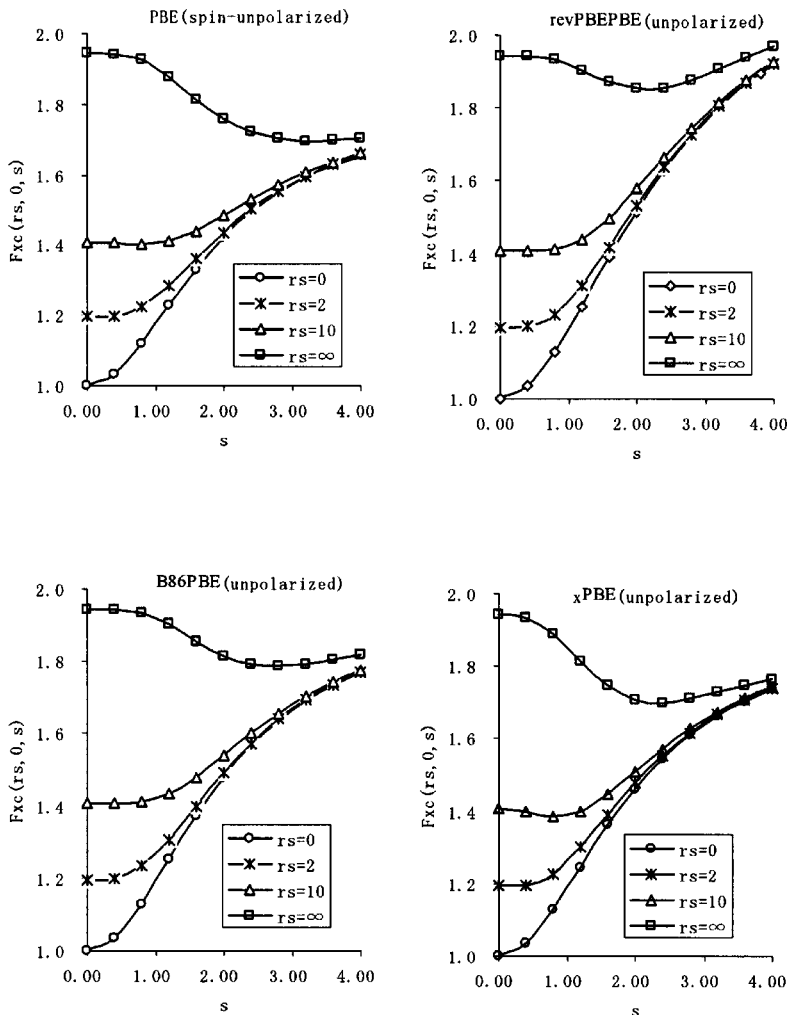

FIG. 2. The enhancement factor $F_{\text{xc}}(r_s, \zeta, s)$, Eq. (8), for the functionals in the PBE family. For all curves the $s \to 0$ asymptotes are 1.0 for $r_s=0.0$, 1.2 for $r_s=2.0$, 1.4 for $r_s=10.0$, and 1.9 for $r_s=\infty$, recovering the LSD limits. The $s \to \infty$ asymptotes are $1+\kappa=1.804$ (PBE), 2.245 (revPBE), 1.9672 (B86), and 1.919\,54 (xPBE) such that the correlation effects vanish. The curves for the limiting cases $r_s=0.0$ and $r_s=\infty$ were generated using $r_s=10^{-6}$ and $r_s=10^6$ a.u., respectively.

TABLE II. Total energies (in a.u.) of Hartree-Fock limit [HF limit (Ref. 41)] for the first 18 atoms from H to Ar and the differential total energies calculated self-consistently by HF and the DFT-exchange-only methods $[\Delta E = E(\text{HF limit}) - E(\text{DFT exchange only})]$. The basis sets used are aug-cc-pVTZ. Mean absolute deviations (MAD) compared to HF limit are given in kcal/mol. The best DFT results are in **boldface**.

Atom	E(HF limit)	ΔE(HF)	ΔE(PBE)	ΔE(revPBE)	ΔE(B86)	ΔE(xPBE)
H	0.5	−0.000 179	−0.005 878	**−0.001 367**	−0.001 850	−0.002 696
He	−2.861 704	−0.000 521	−0.010 211	0.004 762	0.003 450	**0.000 602**
Li	−7.432 730	−0.000 025	−0.023 012	0.001 744	**−0.000 117**	−0.004 867
Be	−14.573 03	−0.000 155	−0.029 480	0.004 756	0.003 732	**−0.003 045**
B	−24.529 06	0.003 112	−0.033 000	0.011 488	0.012 630	**0.003 912**
C	−37.688 64	0.003 171	−0.038 050	0.013 133	0.017 346	**0.006 870**
N	−54.400 96	0.000 202	−0.047 800	0.007 548	0.015 237	**0.003 142**
O	−74.809 42	0.003 563	−0.036 760	0.027 387	0.040 633	**0.026 651**
F	−99.409 32	−0.002 440	−0.035 250	**0.032 964**	0.052 431	0.036 848
Ne	−128.547 10	−0.013 827	−0.042 040	**0.026 822**	0.052 576	0.035 561
Na	−161.858 92	−0.000 883	−0.063 010	**0.013 261**	0.043 306	0.024 278
Mg	−199.614 57	−0.001 219	−0.075 340	**0.005 518**	0.042 417	0.021 613
Al	−241.876 42	0.002 754	−0.092 970	**−0.004 095**	0.038 331	0.015 622
Si	−288.854 33	0.002 298	−0.112 260	−0.017 832	0.030 502	**0.005 991**
P	−340.719 07	−0.002 578	−0.135 610	−0.037 953	0.016 291	**−0.009 989**
S	−397.504 77	0.005 103	−0.146 220	−0.039 430	0.021 413	**−0.006 745**
Cl	−459.481 72	0.004 249	−0.161 760	−0.050 464	0.017 349	**−0.012 546**
Ar	−526.817 90	−0.004 548	−0.184 420	−0.072 649	**0.002 081**	−0.029 504
MAD	⋯	1.8	44.4	13.0	13.6	**8.6**

1.0 for $r_s = 0.0$, 1.2 for $r_s = 2.0$, 1.4 for $r_s = 10.0$, and 1.9 for $r_s = \infty$, recovering the LSD limits. As $s \rightarrow \infty$ the correlation effects vanish. Hence $F_{\text{xc}}(r_s, \zeta, s)$ curves converge to the corresponding $F_x(s)$ curves. All four functionals fulfill the non-curve-crossing condition $F_{\text{xc}}(r_s, s) < F_{\text{xc}}(r_s', s)$ for $r_s < r_s'$ and the positive condition $F_{\text{xc}}(r_s, \zeta, s) > 0$, which were derived from the fundamental scaling inequality involving scaled density $\rho_\lambda E_{\text{xc}}(\rho_\lambda) > \lambda E_{\text{xc}}(\rho)$ for $\lambda > 1$.[44]

Note that to fulfill Eq. (16), H_0 must cancel the logarithmic singularity of ϵ_C^{unif} in the high density limit: $\epsilon_c^{\text{unif}}(r_s, \zeta) \rightarrow g^3[\gamma \ln(r_s) - \omega]$, where $\gamma = (1 - \ln 2)/\pi^2 \approx 0.031\,091$ and $\omega = 0.046\,644$, which are obtained by assuming $\zeta = 0$ in PBE. In xPBE, the optimized α and β lead to $\gamma = \beta^2/(2\alpha) = 0.020\,432$.

Other modifications based on the PBE exchange functional [RPBE (Ref. 13) and mPBE (Ref. 14)] changed the functional form of Eq. (12), and will not be discussed here.

IV. RESULTS AND DISCUSSION

A. Atomic data

Table II compares the total energies (in a.u.) calculated self-consistently by HF and the DFT-exchange-only methods with the total energies in the HF limit[42] for the first 18 atoms from H to Ar. Comparing E(HF) to E(HF limit) the MAD is 1.8 kcal/mol, which may be interpreted as the basis set error remaining with the aug-cc-pVTZ basis for the atomic calculations.

The PBE exchange-only (PBE) calculations lead an unacceptable error (MAD=44.4 kcal/mol). The revPBE (Ref. 12) method relaxed the local Lieb-Oxford bound constraint and optimized κ by fitting exchange-only total atomic energies from He to Ar to the exact exchange-only results from the optimized exchange potential method.[41] The revPBE functional significantly improves upon PBE, leading to

MAD=13.0 kcal/mol. Becke, the first to introduce the exchange functional in Eq. (12),[15] optimized κ and μ by a least-squares fit to the Hartree-Fock exchange energies of 20 atomic systems from H to Ar plus Kr and Xe.[15] This B86 functional leads to much better exchange-only total energies (MAD=13.6) than does PBE. From Table II, we see that xPBE (MAD=8.6 kcal/mol) leads to the best performance of the various exchange functional for atomic calculations. For comparison, we also calculated the exchange-only total energies for the first 18 atoms from H to Ar calculated self-consistently by B88 (Ref. 9) and PW91 (Ref. 10) exchange functionals with aug-cc-pVTZ. As compared to the HF limit,[42] B88 leads to MAD=7.1; while PW91 leads to MAD=12.7 kcal/mol.

Table III presents another way of gauging the quality of an exchange functional. Taking HF exchange energies as a reference, post-DFT calculations with HF densities give MAD for the exchange energies of 46.5 (PBE), 12.9 (revPBE), 11.9 (B86), and 8.6 kcal/mol (xPBE), respectively. Similar calculations lead to MAD=8.3 (B88) and 16.1 kcal/mol (PW91). The MAD associated with PBE is significantly larger than those of the other exchange functionals; however $|\Delta E_x(\text{PBE})|$ increases systematically for larger atoms suggesting that the errors associated with the PBE exchange functional may be systematic.

Table IV summarizes the correlation energies for the first 18 atoms from H to Ar (Ref. 42) and the correlation energies calculated self-consistently by DFT methods. The revPBE and B86PBE functionals share the same correlation functional as does PBE. Thus the slight difference in the correlation energies among these three sets reflects the effect of different densities originating from the different exchange functionals. The PBE correlation functional gives a MAD of 12.4, while the xPBE correlation functional gives a MAD of

TABLE III. Hartree-Fock (HF) exchange energies (in a.u.) of the first 18 atoms from H to Ar and the differential DFT exchange-only exchange energies [$\Delta E_x = E_x(\text{HF}) - E_x(\text{DFT}$ exchange only)], in a.u., DFT energies are calculated with HF densities. The basis sets used are aug-cc-pVTZ. Mean absolute deviations (MADs) are given in kcal/mol. The best DFT results are in **boldface**.

Atom	$E_x(\text{HF})$	$\Delta E_x(\text{PBE})$	$\Delta E_x(\text{revPBE})$	$\Delta E_x(\text{B86})$	$\Delta E_x(\text{xPBE})$
H	−0.312 190	−0.006 528	**−0.001 946**	−0.002 495	−0.003 346
He	−1.025 447	−0.012 149	0.002 939	0.001 498	**−0.001 353**
Li	−1.781 214	−0.023 927	0.001 011	**−0.000 940**	−0.005 713
Be	−2.666 716	−0.031 097	0.003 625	0.002 303	−0.004 531
B	−3.759 184	−0.035 166	0.007 908	0.008 695	**−0.000 081**
C	−5.066 702	−0.041 857	0.008 251	0.012 012	**0.001 452**
N	−6.604 576	−0.054 357	**0.001 972**	0.009 068	−0.003 148
O	−8.204 931	−0.043 737	0.018 561	0.031 180	**0.017 083**
F	−10.031 048	−0.038 310	**0.028 347**	0.047 096	0.031 375
Ne	−12.102 300	−0.041 093	**0.029 166**	0.054 070	0.036 881
Na	−14.017 379	−0.066 965	**0.009 813**	0.039 603	0.020 606
Mg	−15.994 046	−0.079 566	**0.002 201**	0.038 573	0.017 651
Al	−18.079 161	−0.096 917	**−0.009 220**	0.032 816	0.010 013
Si	−20.292 187	−0.116 116	−0.022 850	0.025 023	**0.000 395**
P	−22.640 536	−0.139 566	−0.040 757	**0.012 893**	−0.013 547
S	−25.019 285	−0.151 899	−0.047 844	**0.012 461**	−0.015 837
Cl	−27.530 263	−0.167 157	−0.058 533	**0.008 690**	−0.021 859
Ar	−30.183 224	−0.188 614	−0.075 523	**−0.001 467**	−0.033 234
MAD	⋯	46.5	12.9	11.9	**8.6**

6.5 kcal/mol. Similar calculations lead to MAD=7.3 [BLYP (Refs. 9 and 16)] and 9.1 kcal/mol [PW91 (Ref. 17)].

The exchange-correlation total atomic energies calculated self-consistently with various DFT methods of the PBE family are summarized in Table V. Each MAD is calculated relative to the exact atomic total energies.[42] PBE leads to unacceptable error of 55.5 kcal/mol. MAD (revPBE)=15.4, MAD (B86PBE)=5.0, and MAD (xPBE)=4.1 kcal/mol. Similar calculations lead to MAD [BLYP (Refs. 9 and 16)] =7.6 and MAD [PW91 or GGA II (Refs. 10 and 17)]=4.9 kcal/mol. Although B86PBE, xPBE, and PW91 give the best

results for the atomic calculations, there are error cancellations between the exchange part and the correlation part in these functionals.

B. Bond lengths and bond angles

Table VI summarizes the experimental geometric parameters for a set of 32 molecules gathered by Pople and co-workers[45] and compares the optimization results for the various GGAs. It has long been recognized that LDA (SVWN, Slater exchange functional plus Vosko-Wilk-Nusair

TABLE IV. Correlation energies (in a.u.) for the first 18 atoms from H to Ar (Ref. 41) and the differential correlation energies calculated self-consistently by DFT methods [$\Delta E_c = E_c(\text{Exact}) - E_c(\text{DFT})$]. The basis sets used are aug-cc-pVTZ. Mean absolute deviations (MAD) are given in kcal/mol. The best DFT results are in **boldface**.

Atom	$\Delta E_c(\text{Exact})$	$\Delta E_c(\text{PBE})$	$\Delta E_c(\text{revPBE})$	$\Delta E_c(\text{B86PBE})$	$\Delta E_c(\text{xPBE})$
H	0	0.005 68	0.005 70	0.005 68	**0.005 57**
He	−0.042 02	−0.001 09	−0.001 04	−0.001 08	**−0.000 70**
Li	−0.045 33	**0.005 95**	0.005 99	0.005 98	0.008 75
Be	−0.094 36	−0.009 19	−0.009 08	−0.009 15	**−0.005 46**
B	−0.124 84	−0.012 80	−0.012 68	−0.012 77	**−0.007 34**
C	−0.156 36	−0.013 13	−0.012 99	−0.013 08	**−0.005 46**
N	−0.188 34	−0.010 32	−0.010 15	−0.010 26	**−0.000 12**
O	−0.257 98	−0.025 69	−0.025 52	−0.025 63	**−0.013 43**
F	−0.324 78	−0.036 16	−0.035 95	−0.036 09	**−0.021 35**
Ne	−0.391 20	−0.044 93	−0.044 69	−0.044 85	**−0.027 22**
Na	−0.396 48	−0.026 28	−0.026 26	−0.026 25	**−0.004 65**
Mg	−0.439 43	−0.029 92	−0.029 85	−0.029 88	**−0.005 56**
Al	−0.470 58	−0.026 35	−0.026 26	−0.026 31	**0.001 68**
Si	−0.505 67	−0.022 76	−0.022 62	−0.022 70	**0.008 84**
P	−0.540 93	−0.016 25	−0.016 01	−0.016 14	**0.018 94**
S	−0.606 23	−0.023 66	−0.023 42	−0.023 57	**0.014 38**
Cl	−0.668 28	−0.025 78	−0.025 49	−0.025 68	**0.015 48**
Ar	−0.726 10	−0.022 33	**−0.021 98**	−0.022 20	0.022 31
MAD	⋯	12.4	12.3	12.3	**6.5**

TABLE V. Total atomic energies (in a.u.) of the first 18 atoms from H to Ar. DFT energies are calculated self-consistently with aug-cc-pVTZ. The differences between the exact total atomic energies (Ref. 41) and DFT energies $[\Delta E = E(\text{Exact}) - E(\text{DFT})]$ are given in a.u. Mean absolute deviations (MADs) are given in kcal/mol. The best DFT results are in **boldface**.

Atom	Exact	$\Delta E(\text{PBE})$	$\Delta E(\text{revPBE})$	$\Delta E(\text{B86PBE})$	$\Delta E(\text{xPBE})$
H	0.5	−0.000 197	0.004 334	0.003 834	**0.002 572**
He	−2.903 724	−0.011 302	0.003 717	0.002 866	**−0.001 908**
Li	−7.478 060	−0.017 063	0.007 732	0.005 861	**0.001 258**
Be	−14.667 39	−0.038 642	**−0.004 289**	−0.005 384	−0.012 230
B	−24.653 90	−0.045 320	−0.002 745	**−0.001 669**	−0.009 983
C	−37.845 0	−0.050 820	**−0.001 342**	0.002 792	−0.006 385
N	−54.589 8	−0.058 126	**−0.002 606**	0.004 980	−0.004 629
O	−75.067 4	−0.061 694	**−0.000 287**	0.012 874	0.001 686
F	−99.7341	−0.071 057	−0.005 388	0.013 955	**0.001 941**
Ne	−128.938 3	−0.086 269	−0.017 169	0.008 425	**−0.003 893**
Na	−162.255 4	−0.088 484	−0.012 197	0.017 857	**0.006 268**
Mg	−200.054	−0.104 253	−0.023 330	0.013 537	**0.001 192**
Al	−242.347	−0.117 679	−0.030 722	0.011 719	**−0.000 328**
Si	−289.360	−0.133 426	−0.040 976	0.007 318	**−0.004 385**
P	−341.260	−0.150 856	−0.052 961	**0.001 146**	−0.010 162
S	−398.111	−0.168 225	−0.065 079	**−0.004 336**	−0.016 308
Cl	−460.150	−0.185 016	−0.077 310	**−0.009 657**	−0.021 772
Ar	−527.544	−0.202 749	−0.090 625	**−0.016 118**	−0.028 132
MAD	⋯	55.5	15.4	5.0	**4.1**

correlation functional) frequently gives bond lengths which are too long, while this trend is unaltered with the more elaborate GGA such as BLYP.[45] Our results show that functionals of the PBE family give bond lengths which are consistently long, similar to LDA (SVWN) and BLYP. For H_2 the bond length (0.741 Å) is overestimated by 0.0099 (PBE), 0.0071 (revPBE), 0.0072 (B86PBE), and 0.0069 Å (xPBE). For the other 25 X-H bonds in Table VI, the bond lengths are too long by 0.0113 (PBE), 0.0123 (revPBE), 0.0110 (B86PBE), and 0.0103 Å (xPBE). For bonds between non-hydrogen atoms (X-Y), the situation is worse. The MADs are increased to 0.0135 (PBE), 0.0181 (revPBE), 0.0155 (B86PBE), and 0.0150 Å (xPBE).

Table VI also includes 18 bond angles and dihedral angles. All four functionals lead to bond angles which are too small. An exception from this trend is α (OOH) of HOOH, for which the optimized results are larger than the experimental value by $\sim 5°$.

Based on the data in Table VI, we find that the MADs for the prediction of bond lengths follow xPBE (0.012 Å) =PBE (0.012)<B86PBE (0.013)<revPBE (0.015), while the MADs for the prediction of bond angles follow PBE (1.728°)<xPBE (1.779)<B86PBE (1.809)<revPBE (1.890).

C. Heats of formation

Table VII lists the experimental heats of formation (298 K) for the extended $G2$ set of 148 molecules and compares the results for the various GGAs.[27–28] The MAD deviations from experiment (theory-expt.) are presented: PBE=16.9 kcal/mol, revPBE=7.3, B86PBE=7.9 and xPBE=8.0. PBE leads to a MAD too high to be useful for thermochemistry, with a clear tendency to overbind (many more negative deviations than positive deviations). In PBE, the maximum negative deviation (−50.5 kcal/mol) occurs for C_2F_4, while

the maximum positive deviation (10.1 kcal/mol) occurs for Si_2H_6. The revPBE functional significantly improves the overall accuracy of PBE (MAD=7.3 kcal/mol), leading to an error distribution ranging from −25.4 (NO_2) to 29.7 kcal/mol (SiF_4), thus overcorrecting the overbinding tendency of PBE, B86PBE, and xPBE show comparable performance, with MAD≈8 kcal/mol and an error distribution ranging from −32 to 19 kcal/mol. In comparison, PW91 leads to MAD=17.8,[44] while BLYP leads to MAD=7.1 kcal/mol (Ref. 28) for the extended $G2$ set.

In PBE there is a self-correlation energy for the hydrogen atom (3.6 kcal/mol for H). This situation is not improved in xPBE (See Table IV). For the inorganic hydrides (X_nH_m, X=H, Li, N, O, F, Si, P S, Cl; n=1, 2; m=1–6), all methods show a similar performance, with MAD=5.5 (PBE), 4.9 (revPBE), 4.7 (B86PBE), and 5.4 (xPBE) for this subset.

The performance of PBE for larger hydrocarbons (No. 78–94 in Table VII) is less satisfactory. The MAD of this subset is 22.0 kcal/mol, with the maximum error of −44.1 kcal/mol for the aromatic molecule benzene. The revPBE functional performs much better, with MAD=10.7 kcal/mol. The maximum error (24.1 kcal/mol) occurs at isobutane. For benzene, revPBE deviates from experiment by 6.3 kcal/mol. B86PBE (MAD=5.5) and xPBE (MAD=5.8) are the best for this subset, with a maximum error of −14.7 kcal/mol at benzene.

For a subset of substituted hydrocarbons (No. 95–136 in Table VII), the performance of PBE is also less satisfactory, showing a tendency toward large overbinding. The MAD of this subset is 22.9 kcal/mol, with the maximum error of −49.9 kcal/mol for pyridine. The revPBE functional significantly improves over PBE, with the MAD being reduced to 6.8 kcal/mol. The maximum error (18.8 kcal/mol) occurs at isopropanol. B86PBE and xPBE have a similar accuracy,

TABLE VI. Experimental geometries (Ref. 45). Bond distances in angstroms, bond and dihedral angles in degrees. DFT geometries optimizations are performed with aug-cc-pVTZ($-f$). The best DFT results are in **boldface.**

No.	Molecule	Geometric parameters	Expt.	PBE	revPBE	B86PBE	xPBE
1	H_2	r(HH)	0.741	0.751	**0.748**	**0.748**	**0.748**
2	LiH	r(LiH)	1.595	1.606	1.612	1.606	**1.605**
3	BeH	r(BeH)	1.343	1.357	1.359	1.356	**1.355**
4	CH	r(CH)	1.120	1.136	1.138	1.136	**1.135**
5	CH_2 ($^3B_1$)	r(CH)	1.078	1.085	1.086	**1.084**	**1.084**
		a(HCH)	136.0	**135.7**	135.1	135.4	135.4
6	CH_2 ($^1A_1$)	r(CH)	1.111	1.122	1.124	1.122	**1.121**
		a(HCH)	102.4	**100.8**	100.7	**100.8**	**100.8**
7	CH_3	r(CH)	1.079	1.086	1.087	**1.085**	**1.085**
8	CH_4	r(CH)	1.086	1.096	1.097	1.096	**1.095**
9	NH	r(NH)	1.045	1.050	1.051	1.050	**1.049**
10	NH_2	r(NH)	1.024	1.037	1.038	1.037	1.036
		a(HNH)	103.4	102.3	102.1	102.2	102.3
11	NH_3	r(NH)	1.012	1.023	1.024	1.023	1.022
		a(HNH)	106.0	106.0	105.7	105.9	105.9
12	OH	r(OH)	0.971	0.985	0.985	0.984	0.984
13	H_2O	r(OH)	0.959	0.971	0.971	0.971	0.970
		a(HOH)	103.9	104.1	103.9	104.0	104.1
14	HF	r(HF)	0.917	0.932	0.932	0.932	0.932
15	Li_2	r(LiLi)	2.670	2.728	2.750	2.732	2.733
16	LiF	r(LiF)	1.564	1.586	1.597	1.591	1.590
17	C_2H_2	r(CC)	1.203	1.207	1.210	1.208	1.207
		r(CH)	1.061	1.070	1.070	1.069	1.069
18	$H_2C{=}CH_2$	r(CC)	1.339	1.333	1.337	1.335	1.334
		r(CH)	1.085	1.091	1.092	1.091	1.090
		a(HCH)	117.8	116.6	116.5	116.5	116.5
19	$H_3C{-}CH_3$	r(CC)	1.526	1.530	1.537	1.534	1.533
		r(CH)	1.088	1.099	1.100	1.098	1.098
		a(HCH)	107.4	107.6	107.6	107.6	107.6
20	CN	r(CN)	1.172	1.175	1.178	1.176	1.175
21	HCN	r(CN)	1.153	1.159	1.162	1.160	1.159
		r(CH)	1.065	1.075	1.075	1.074	1.073
22	CO	r(CO)	1.128	1.138	1.141	1.140	1.139
23	HCO	r(CO)	1.117	1.184	1.188	1.186	1.185
		r(CH)	1.110	1.134	1.135	1.133	1.132
		a(HCO)	127.4	123.9	123.9	123.9	123.9
24	$H_2C{=}O$	r(CO)	1.208	1.210	1.214	1.212	1.212
		r(CH)	1.116	1.117	1.118	1.116	1.116
		a(HCO)	116.5	116.1	116.0	116.1	116.0
25	$CH_3{-}OH$	r(CO)	1.421	1.431	1.439	1.437	1.436
	(H_a in-plane,	r(CH_a)	1.093	1.096	1.097	1.096	1.095
	H_b out-of-						
	plane)						
		r(CH_b)	1.093	1.103	1.103	1.102	1.101
		r(OH)	0.963	0.970	0.970	0.970	0.970
		a(OCH_a)	107.0	106.7	106.6	106.6	106.6
		a(COH)	108.0	107.9	107.6	107.7	107.8
		a(H_bCH_b)	108.5	109.0	109.1	109.1	109.1
26	N_2	r(NN)	1.098	1.103	1.106	1.105	1.104
27	$H_2N{-}NH_2$	r(NN)	1.447	1.447	1.458	1.454	1.452
		r(NH_b)	1.008	1.025	1.026	1.025	1.024
		r(NH_a)	1.008	1.021	1.022	1.021	1.020
		a(NNH_b)	113.3	111.5	111.1	111.2	111.3
		a(NNH_a)	109.2	106.7	106.2	106.4	106.5
		a(H_aNH_b)	109.2	106.9	106.5	106.7	106.8
		d(H_aNNH_b)	88.90	90.40	90.37	90.44	90.42
28	NO	r(NO)	1.151	1.160	1.164	1.162	1.162
29	O_2	r(OO)	1.207	1.225	1.230	1.228	1.228
30	HO-OH	r(OO)	1.475	1.468	1.476	1.475	1.474
		r(OH)	0.950	0.977	0.977	0.977	0.976
		a(OOH)	94.80	99.93	99.80	99.82	99.87
		d(HOOH)	120.0	111.7	111.5	111.7	111.8
31	F_2	r(FF)	1.417	1.415	1.422	1.421	1.421
32	CO_2	r(CO)	1.162	1.172	1.175	1.173	1.173
MAD(distance)			$\cdots$	**0.012**	0.015	0.013	**0.012**
MAD(angle)				**1.728**	1.890	1.809	1.779

TABLE VII. Experimental heats of formation (kcal/mol 298 K) for the $G2$ test set (148 molecules) (Refs. 27 and 28) and the deviations (theory-expt.) obtained from PBE, revPBE, B86PBE, and xPBE using aug-cc-pVTZ, basis sets. $G2$ geometries (Refs. 27 and 28) are used in the DFT calculations. The best DFT results are in **boldface.**

No.	Molecule	Expt.	PBE	revPBE	B86PBE	xPBE
1	H_2	0.00	4.578	**3.657**	4.072	5.135
2	LiH	33.30	4.455	4.632	**4.244**	5.358
3	BeH	81.70	−5.806	**−5.044**	−5.585	−5.314
4	CH	142.50	−0.900	0.578	**−0.288**	0.370
5	CH_2 ($^3B_1$)	93.70	−4.468	**−0.722**	−2.226	−1.571
6	CH_2 ($^1A_1$)	102.75	**1.649**	5.242	3.489	4.599
7	CH_3	35.00	−3.410	2.513	**−0.080**	1.193
8	CH_4	−17.90	**−0.852**	7.332	3.892	5.629
9	NH	85.20	−5.039	**−3.104**	−4.327	−3.527
10	NH_2	45.10	−7.162	**−2.564**	−4.992	−3.590
11	NH_3	−10.97	−4.610	2.989	**−0.533**	1.317
12	OH	9.40	−3.597	**−0.486**	−1.876	−1.259
13	H_2O	−57.80	−2.132	4.463	**1.836**	3.004
14	HF	−65.14	−1.307	2.584	**1.184**	1.720
15	SiH_2 ($^1A_1$)	65.20	**3.541**	5.732	4.723	6.044
16	SiH_2 ($^3B_1$)	86.20	−0.889	0.708	**0.350**	1.326
17	SiH_3	47.90	**2.867**	5.817	4.658	6.361
18	SiH_4	8.20	**8.185**	12.508	10.624	12.960
19	PH_2	33.10	−1.845	0.900	**−0.243**	1.078
20	PH_3	1.30	**2.358**	6.878	5.088	6.906
21	H_2S	−4.90	**0.335**	4.382	3.048	4.005
22	HCl	−22.06	**−0.440**	1.948	1.261	1.663
23	Li_2	51.60	**4.032**	4.586	4.132	4.867
24	LiF	−80.10	−1.749	3.352	**0.634**	0.946
25	C_2H_2	54.19	−9.509	3.343	−2.296	**−1.837**
26	$H_2C{=}CH_2$	12.54	−9.092	6.147	**−0.386**	1.073
27	$H_3C{-}CH_3$	−20.08	−6.075	11.617	**4.229**	6.630
28	CN	104.90	−14.476	**−5.411**	−9.820	−9.720
29	HCN	31.50	−13.436	**−2.380**	−7.615	−7.002
30	CO	−26.42	−10.309	**−0.981**	−4.945	−4.746
31	HCO	10.00	−17.302	**−6.414**	−10.973	−10.492
32	$H_2C{=}O$	−25.96	−13.102	**−0.673**	−5.881	−4.912
33	$CH_3{-}OH$	−48.00	−8.815	6.899	**0.429**	2.369
34	N_2	0.00	−13.416	**−4.133**	−8.940	−8.289
35	$H_2N{-}NH_2$	22.79	−15.114	**1.240**	−6.255	−3.560
36	NO	21.58	−19.198	**−9.934**	−14.123	−13.671
37	O_2	0.00	−22.832	**−14.032**	−17.355	−17.192
38	HO{-}OH	−32.53	−13.597	**−0.424**	−5.790	−4.402
39	F_2	0.00	−13.398	**−6.552**	−9.194	−9.156
40	CO_2	−94.05	−29.093	**−11.453**	−18.573	−18.580
41	Na_2	33.96	−1.087	**−0.168**	−0.953	−0.283
42	Si_2	139.87	−3.769	**0.290**	−1.203	−1.165
43	P_2	34.31	−4.506	1.545	−0.983	**−0.485**
44	S_2	30.74	−13.137	**−6.932**	−9.115	−9.307
45	Cl_2	0.00	−7.044	**−1.759**	−3.559	−3.636
46	NaCl	−43.56	**2.845**	5.526	4.330	4.866
47	SiO	−24.64	−3.444	4.747	**1.070**	1.578
48	CS	66.90	−8.283	**−1.070**	−3.986	−4.031
49	SO	1.20	−15.495	**−7.533**	−10.636	−10.550
50	ClO	24.19	−16.727	**−9.685**	−12.442	−12.337
51	ClF	−13.24	−10.654	**−4.177**	−6.594	−6.571
52	$H_3Si{-}SiH_3$	19.10	**10.137**	20.096	15.979	19.309
53	CH_3Cl	−19.56	−6.436	5.009	**0.494**	1.559
54	$H_3C{-}SH$	−5.50	−5.221	8.114	**2.875**	4.494
55	HOCl	−17.80	−10.995	**−1.661**	−5.258	−4.636
56	SO_2	−70.95	−20.517	**−4.020**	−10.512	−10.148
57	BF_3	−271.41	−13.075	7.874	**−0.927**	−1.122
58	BCl_3	−96.30	−15.428	**0.757**	−5.310	−5.979
59	AlF_3	−289.03	**1.367**	18.032	10.664	10.669
60	$AlCl_3$	−139.72	**−1.568**	10.908	6.121	6.322
61	CF_4	−223.04	−30.625	**−1.715**	−12.731	−12.662
62	CCl_4	−22.94	−22.615	**1.143**	−7.536	−8.367
63	C{=}O{=}S	−33.08	−27.202	**−11.588**	−17.720	−17.967
64	CS_2	27.95	−23.977	**−10.253**	−15.486	−15.895

TABLE VII. (*Continued.*)

No.	Molecule	Expt.	PBE	revPBE	B86PBE	xPBE
65	COF$_2$	−152.70	−23.929	**−0.779**	−9.794	−9.763
66	SiF$_4$	−385.98	**4.403**	29.681	18.995	19.206
67	SiCl$_4$	−158.40	**−3.169**	16.345	9.202	9.202
68	N$_2$O	19.61	−39.088	**−21.781**	−29.403	−28.833
69	ClNO	12.36	−33.577	**−19.938**	−25.754	−25.187
70	NF$_3$	−31.57	−41.792	**−20.875**	−29.215	−28.605
71	PF$_3$	−229.07	−10.472	9.784	**1.421**	1.933
72	O$_2$	34.10	−37.418	**−20.848**	−27.340	−26.833
73	F$_2$O	5.86	−30.002	**−16.170**	−21.638	−21.370
74	ClF$_3$	−37.97	−39.619	**−20.071**	−27.631	−27.674
75	C$_2$F$_4$	−157.40	−50.537	**−14.664**	−28.749	−29.108
76	C$_2$Cl$_4$	−2.97	−36.371	**−5.017**	−16.938	−18.370
77	CF$_3$CN	−118.40	−44.209	**−8.216**	−23.057	−23.055
78	C$_3$H$_4$ (propyne)	44.20	−16.917	**5.596**	−3.991	−2.917
79	C$_3$H$_4$ (allene)	45.50	−21.750	**0.921**	−8.733	−7.621
80	C$_3$H$_4$ (cyclopropene)	66.20	−19.823	**3.355**	−6.088	−5.364
81	C$_3$H$_6$ (propylene)	4.78	−14.665	10.469	**−0.150**	1.957
82	C$_3$H$_6$ (cyclopropane)	12.70	−16.607	9.461	−1.096	**0.632**
83	C$_3$H$_6$ (propane)	−25.00	−10.538	17.102	**5.565**	8.643
84	C$_4$H$_6$ (butadiene)	26.30	−23.736	8.754	−5.082	**−3.284**
85	C$_4$H$_6$ (2-butyne)	34.80	−23.151	9.014	−4.526	**−2.833**
86	C$_4$H$_6$ (methylene cyclopropane)	47.90	−29.508	**3.758**	−9.868	−8.501
87	C$_4$H$_6$ (bicyclobutane)	51.90	−26.259	8.069	−5.547	**−4.496**
88	C$_4$H$_6$ (cyclobutene)	37.40	−24.075	9.631	−4.062	**−2.388**
89	C$_4$H$_8$ (cyclobutane)	6.80	−20.801	15.535	**0.805**	3.359
90	C$_4$H$_8$ (isobutene)	−4.00	−19.118	16.213	**1.368**	4.094
91	C$_4$H$_{10}$ (trans butane)	−30.00	−14.851	22.737	**7.056**	10.806
92	C$_4$H$_{10}$ (isobutane)	−32.07	−13.934	24.104	**8.212**	11.886
93	C$_5$H$_8$ (spiropentane)	44.30	−33.677	10.475	−7.257	**−5.639**
94	C$_6$H$_6$ (benzene)	19.74	−44.085	**6.258**	−14.741	−13.723
95	H$_2$CF$_2$	−107.71	−16.299	**1.510**	−5.574	−4.691
96	HCF$_3$	−166.60	−23.537	**−0.192**	−9.266	−8.800
97	H$_2$CCl$_2$	−22.83	−11.713	3.453	−2.348	**−1.915**
98	HCCl$_3$	−24.66	−17.132	**2.120**	−5.063	−5.243
99	H$_3$C—NH$_2$ (methylamine)	−5.50	−9.959	7.066	**−0.368**	2.192
100	CH$_3$—CN (methyl cyanide)	18.00	−20.581	**0.117**	−9.052	−7.820
101	CH$_3$—NO$_2$ (nitromethane)	−17.80	−42.268	−12.908	−25.078	−23.417
102	CH$_3$—O—N=O (methyl nitrite)	−15.90	−39.770	−10.840	−23.020	−21.082
103	CH$_3$—SiH$_3$ (methyl silane)	−7.00	**4.497**	18.414	12.530	15.508
104	HCOOH (formic acid)	−90.50	−23.343	**−2.306**	−10.846	−9.772
105	HCOOCH$_3$ (methyl formate)	−85.00	−29.267	**1.516**	−11.206	−9.383
106	CH$_3$CONH$_2$ (acetamide)	−57.00	−29.514	**3.039**	−10.777	−8.473
107	CH$_2$—NH—CH$_2$ (aziridine)	30.20	−21.528	**3.303**	−7.046	−5.058
108	NCCN (cyanogen)	73.30	−36.243	**−12.904**	−23.829	−23.733
109	(CH$_3$)$_2$NH (dimethylamine)	−4.40	−15.036	11.947	**0.340**	3.601
110	CH$_3$—CH$_2$—NH$_2$ (*trans* ethylamine)	−11.30	−15.600	11.421	**−0.186**	3.027
111	H$_2$C=C=O (ketene)	−11.35	−27.334	**−7.114**	−15.515	−14.955
112	H$_2$C—O—CH$_2$ (oxirane)	−12.57	−21.168	**2.008**	−7.277	−5.847
113	CH$_3$CHO (acetaldehyde)	−39.70	−19.248	**3.162**	−6.161	−4.597
114	O=CH—CH=O (glyoxal)	−50.70	−31.633	**−4.935**	−16.055	−15.295
115	CH$_3$—CH$_2$OH (ethanol)	−56.21	−13.216	12.485	**1.847**	4.454
116	CH$_3$—O—CH$_3$ (dimethylether)	−44.00	−14.305	11.186	**0.547**	3.231
117	CH$_2$—S—CH$_2$ (thiooxirane)	19.60	−17.041	4.350	−3.978	**−2.979**
118	CH$_3$CH$_3$SO (dimethyl sulfoxide)	−36.20	−19.784	11.471	−1.217	**1.151**
119	CH$_3$—CH$_2$—SH (ethanethiol)	−11.10	−9.332	13.942	**4.568**	6.830
120	CH$_3$—S—CH$_3$ (dimethyl sulphide)	−8.90	−10.640	12.347	**3.068**	5.331
121	H$_2$C=CHF	−33.20	−19.563	**0.776**	−7.655	−6.661
122	CH$_3$—CH$_2$—Cl (ethyl chloride)	−26.80	−10.966	10.457	**1.769**	3.514
123	H$_2$C=CHCl (vinyl chloride)	8.90	−19.513	**−0.568**	−8.305	−7.554
124	H$_2$C=CHCN (acrylonitrile)	43.20	−27.966	**−0.104**	−12.427	−11.471
125	CH$_3$—CO—CH$_3$ (acetone)	−51.93	−24.095	8.474	−5.070	**−2.863**
126	CH$_3$COOH (acetic acid)	−103.40	−27.793	**3.287**	−9.416	−7.708
127	CH$_3$COF (acetyl fluoride)	−105.70	−27.814	**0.008**	−11.306	−10.225
128	CH$_3$COCl (acetyl chloride)	−58.00	−27.286	**−0.934**	−11.544	−10.630
129	CH$_3$CH$_2$CH$_2$Cl (propyl chloride)	−31.52	−15.542	15.762	**2.957**	5.366
130	(CH$_3$)$_2$CH—OH (isopropanol)	−65.20	−17.310	18.780	**3.796**	7.008

TABLE VII. (*Continued.*)

No.	Molecule	Expt.	PBE	revPBE	B86PBE	xPBE
131	C_2H_5—O—CH_3 (methyl ethyl ether)	−51.70	−19.170	16.297	**1.505**	4.822
132	$(CH_3)_3N$ (trimethylamine)	−5.70	−19.884	17.640	**1.573**	5.534
133	C_4H_4O (furan)	−8.30	−39.871	**0.718**	−15.806	−14.898
134	C_4H_4S (thiophene)	27.50	−34.987	**3.260**	−12.047	−11.618
135	C_4H_4NH (pyrrole)	25.90	−41.303	**1.151**	−16.543	−15.115
136	C_5H_5N (pyridine)	33.60	−49.860	**−0.806**	−21.587	−20.339
137	SH	34.18	−1.147	0.800	**0.114**	0.631
138	CCH	135.10	−10.080	**0.537**	−4.094	−4.248
139	C_2H_3 ($^2A'$)	71.60	−13.700	**−0.289**	−6.077	−5.140
140	CH_3CO ($^2A'$)	−2.40	−23.816	**−3.220**	−11.809	−10.694
141	H_2COH (^2A)	−4.08	−13.259	**0.800**	−5.012	−3.541
142	CH_3O ($^2A'$)	4.10	−12.861	**0.068**	−5.394	−4.024
143	CH_3CH_2O ($^2A''$)	−3.70	−14.278	8.585	−1.032	**0.992**
144	CH_3S ($^2A'$)	29.80	−8.674	2.733	−1.897	**−0.718**
145	C_2H_5 ($^2A'$)	28.90	−9.749	5.909	**−0.701**	1.217
146	$(CH_3)_2CH$ ($^2A'$)	21.50	−15.629	9.997	**−0.730**	1.832
147	$(CH_3)_3C$	12.30	−19.811	16.060	**1.074**	4.346
148	NO_2	7.91	−42.513	**−25.374**	−32.455	−32.021
MAD		⋯	16.9	**7.3**	7.9	8.0

leading to MAD~8.6 kcal/mol, with a maximum error of −25 kcal/mol at nitromethane.

For the subset of radicals (No. 138–148 in Table VII), PBE leads to MAD=16.8 kcal/mol, with a maximum error of −42.5 kcal/mol at NO_2. Errors for the other three functionals are significantly smaller, with MAD=6.7 (revPBE), 6.4 (B86PBE), and 6.3 (xPBE). All these functionals have problems for NO_2, leading to errors of −25.4 (revPBE), −32.5 (B86PBE), and −32.0 (xPBE).

The fluorine- and chlorine-containing compounds of the *G*2 set are generally most difficult to describe well. This subset of compounds (No. 57–77 in Table VII) leads to MADs of 23.7 kcal/mol (PBE), 11.9 (revPBE), 15.1 (B86PBE), and 15.2 kcal/mol (xPBE). The largest errors encountered are −50.5 (C_2F_4, PBE), 29.7 (SiF_4, revPBE), −29.4 (N_2O, B86PBE), and −29.1 kcal/mol (C_2F_4, xPBE).

We should point out that although the modified versions of PBE generally improve the accuracy for the thermochemistry, there are cases where the results get considerably worse. For example, PBE overbinds $SiCl_4$ by 3.2 kcal/mol, while it is underbound by 16.3 (revPBE) and 9.2 (B86PBE, xPBE). Perdew *et al.* have criticized that revPBE improves the energetics of multiple bonds by worsening many single bonds.[46] This tendency is seen clearly in the data of Table VII.

D. Ionization potentials, electron affinities, and proton affinities

Table VIII lists the experimental ionization potentials (IPs) and the theoretical deviations from experiments for the 18 atoms and 24 molecules in the *G*2 set;[27,29] while Table IX lists the results of electron affinities (EA) for the 7 atoms and 18 molecules in the *G*2 set.[27,29] We calculated IP and EA as energy differences between the neutral species and the corresponding ionic species. Very accurate experimental IPs for atoms are known providing a good test of the ability of the functionals to handle positively charged systems. For the

atomic systems, the MADs are 0.159 eV (PBE), 0.136 (revPBE), 0.159 (B86PBE), and 0.149 (xPBE). For the molecular systems, the MADs are 0.153 eV (PBE), 0.189 (revPBE), 0.156 (B86PBE), and 0.180 (xPBE). The MADs for the total 42 systems are 0.156 (PBE), 0.166 (revPBE), 0.158 (B86PBE), and 0.167 (xPBE). The IP of O is a problem for all four functionals. PW91 leads to MAD=0.164,[46] while BLYP leads to MAD=0.187 kcal/mol (Refs. 29 and 46) for the same set.

There has been some debate in the literature, concerning whether DFT methods are suitable for calculating electron affinities.[47–50] On one hand, the "self-interaction error" causes the Kohn-Sham orbital energies to be shifted upwards artificially, leading to positive (unstable) orbital energies for the highest occupied orbitals of an anion. On the other hand, an artificial stabilization is provided by employing a finite basis sets with functions localized at the anion.

Actual numerical calculations demonstrate that DFT methods predict electron affinities with an accuracy comparable to conventional *ab initio* calculations.[30,50] For the atomic systems, the MAD are 0.130 eV (PBE), 0.071 (revPBE), 0.119 (B86PBE), and 0.081 (xPBE). All four functionals perform significantly better for the second low atoms.

For the molecular systems, the MAD are 0.090 eV (PBE), 0.098 (revPBE), 0.091 (B86PBE), and 0.093 (xPBE). The EA of C and CH are problematic for PBE, while EA of Cl_2 is problematic for revPBE, B86PBE, and xPBE. The MAD for the total 25 systems are 0.101 (PBE), 0.091 (revPBE), 0.099 (B86PBE), and 0.091 (xPBE) eV. For PW91 and BLYP, similar calculations lead to 0.141 (PW91) and 0.106 (BLYP).[29,46]

Table X lists the proton affinities PAs at 0 K for the eight cases in the *G*2 set and the MAD (theory-expt) obtained from PBE, revPBE, B86PBE, and xPBE. PBE leads to MAD =1.45 kcal/mol with maximum negative deviation being −3.98 kcal/mol. PAs are always underestimated in PBE as shown by the lack of any positive deviations with this func-

TABLE VIII. Ionization potentials (in eV) at 0 K of the 42 systems in $G2$ (Refs. 7 and 29) and the deviations (theory-expt) obtained from PBE, revPBE, B86PBE, and xPBE using aug-cc-pVTZ basis sets. $G2$ geometries (Refs. 27 and 28) are used in the DFT calculations. The best DFT results are in **boldface**.

No.	System	Expt.	PBE	revPBE	B86PBE	xPBE
1	$H \rightarrow H^+$	13.60	**0.00**	0.12	0.10	0.08
2	$He \rightarrow He^+$	24.59	-0.14	0.02	**0.01**	-0.03
3	$Li \rightarrow Li^+$	5.39	**0.18**	0.20	0.22	0.19
4	$Be \rightarrow Be^+$	9.32	-0.32	-0.30	-0.27	-0.33
5	$B \rightarrow B^+$	8.30	0.37	**0.34**	0.39	0.36
6	$C \rightarrow C^+$	11.26	0.28	**0.22**	0.28	0.25
7	$N \rightarrow N^+$	14.54	0.20	**0.12**	0.18	0.15
8	$O \rightarrow O^+$	13.61	0.46	**0.38**	0.50	0.44
9	$F \rightarrow F^+$	17.42	0.26	**0.14**	0.25	0.21
10	$Ne \rightarrow Ne^+$	21.56	0.15	**0.01**	0.11	0.08
11	$CH_4 \rightarrow CH_4^+$	12.62	-0.24	-0.28	**-0.22**	-0.27
12	$NH_3 \rightarrow NH_3^+$	10.18	**-0.01**	-0.08	-0.02	-0.07
13	$OH \rightarrow OH^+$	13.01	0.16	**0.07**	0.16	0.11
14	$H_2O \rightarrow H_2O^+$	12.62	**-0.03**	-0.12	-0.04	-0.09
15	$HF \rightarrow HF^+$	16.04	0.03	-0.08	**0.00**	-0.04
16	$Na \rightarrow Na^+$	5.14	0.21	**0.16**	0.22	0.20
17	$Mg \rightarrow Mg^+$	7.65	-0.03	-0.09	**-0.02**	-0.08
18	$Al \rightarrow Al^+$	5.98	0.09	0.10	0.11	**0.07**
19	$Si \rightarrow Si^+$	8.15	0.05	0.03	0.06	**0.02**
20	$P \rightarrow P^+$	10.49	**0.00**	-0.03	**0.00**	-0.04
21	$S \rightarrow S^+$	10.36	0.07	0.04	0.09	**0.03**
22	$Cl \rightarrow Cl^+$	12.97	**0.01**	-0.05	**0.01**	-0.04
23	$Ar \rightarrow Ar^+$	15.76	**-0.04**	-0.10	-0.05	-0.09
24	$SiH_4 \rightarrow SiH_4^+$	11.00	-0.30	-0.35	**-0.29**	-0.35
25	$PH \rightarrow PH^+$	10.15	0.10	0.08	0.11	**0.06**
26	$PH_2 \rightarrow PH_2^+$	9.82	0.17	0.14	0.18	**0.13**
27	$PH_3 \rightarrow PH_3^+$	9.87	**-0.08**	-0.14	**-0.08**	-0.13
28	$SH \rightarrow SH^+$	10.37	**0.01**	-0.03	0.02	-0.04
29	$H_2S \rightarrow H_2S^+(^2B_1)$	10.47	**-0.10**	-0.15	**-0.10**	-0.15
30	$H_2S \rightarrow H_2S^+(^2A_1)$	12.78	-0.22	-0.26	**-0.21**	-0.26
31	$HCl \rightarrow HCl^+$	12.75	**-0.06**	-0.12	-0.07	-0.12
32	$C_2H_2 \rightarrow C_2H_2^+$	11.40	**-0.16**	-0.27	-0.19	-0.23
33	$C_2H_4 \rightarrow C_2H_4^+$	10.51	**-0.10**	-0.21	-0.13	-0.18
34	$CO \rightarrow CO^+$	14.01	-0.14	-0.20	**-0.13**	-0.19
35	$N_2 \rightarrow N_2^+(^2\Sigma_g)$	15.58	**-0.18**	-0.27	-0.19	-0.24
36	$N_2 \rightarrow N_2^+(^2\Pi_u)$	16.70	**-0.13**	-0.28	0.18	-0.22
37	$O_2 \rightarrow O_2^+$	12.07	0.40	**0.33**	0.40	0.36
38	$P_2 \rightarrow P_2^+$	10.53	0.26	**0.21**	0.26	**0.21**
39	$S_2 \rightarrow S_2^+$	9.36	0.10	0.09	0.12	**0.07**
40	$Cl_2 \rightarrow Cl_2^+$	11.50	-0.35	-0.38	**-0.34**	-0.39
41	$ClF \rightarrow ClF^+$	12.66	-0.30	-0.34	**-0.29**	-0.33
42	$CS \rightarrow CS^+$	11.33	-0.03	-0.06	**-0.01**	-0.08
	MAD	$\cdots$	**0.156**	0.166	0.158	0.167

tional. The MAD for these eight systems are 1.19 (revPBE), 1.08 (B86PBE), and 1.07 kcal/mol (xPBE). For comparison, the MAD=1.43 for PW91 and 1.96 for BLYP.[29,46]

E. Bonding properties of rare-gas dimers

Rare-gas dimers are the least ambiguous test molecules for London dispersion or van der Waals attraction interactions. Table XI summarizes the bonding properties of He_2, Ne_2, and Ar_2 calculated with different flavors of DFT functionals. Although the B88 exchange functional is very successful for describing covalent bonds, it fails to describe van der Waals interactions.[46,51,52] Thus every DFT method using the B88 exchange functional (pure or hybrid) gives unbounded rare-gas dimers; while every DFT method using the PW91 exchange functional severely overbinds the He_2 and

Ne_2 rare-gas dimers.[46] Adamo and Barone modified PW91 (Ref. 21) by fitting the differential exchange energies of rare-gas dimers to HF values, thus removing most of the overbinding tendency of PW91. Their mPWPW model yields $R(He\text{-}He) = 3.14$ Å and $\Delta E(He\text{-}He) = 0.069$ kcal/mol,[21] as compared to the PW91 values of $R(He\text{-}He) = 2.645$ Å and $\Delta E(He\text{-}He) = 0.231$ kcal/mol (Ref. 21) and the experimental data of $R(He\text{-}He) = 2.970$ Å $\Delta E(He\text{-}He) = 0.022$ kcal/mol.[43]

The PBE functional gives a better description of rare-gas dimers than PW91 or BLYP.[46,53,54] For Ne_2, PBE yields $R = 3.097$ Å and $\Delta E = 0.111$ kcal/mol, which compares well with the experimental data of $R(Ne\text{-}Ne) = 3.091$ Å, $\Delta E(Ne\text{-}Ne) = 0.084$ kcal/mol.[43] But PBE still overestimates $\Delta E(He\text{-}He)$ by 236% and underestimates $\Delta E(Ar\text{-}Ar)$ by 56%. The revPBE functional gives satisfac-

TABLE IX. Electron affinities (in eV) at 0 K of 25 systems of $G2$ (Refs. 7 and 29) and the deviations (theory-expt.) obtained from PBE, revPBE, B86PBE, and xPBE using aug-cc-pVTZ basis set. $G2$ geometries (Refs. 27 and 28) are used in the DFT calculations. The best DFT results are in boldface.

No.	System	Expt.	PBE	revPBE	B86PBE	xPBE
1	$C \leftarrow C^-$	1.26	0.29	**0.23**	0.27	0.24
2	$CH \leftarrow CH^-$	1.24	0.29	**0.22**	0.27	0.23
3	$^3CH_2 \leftarrow CH_2^-$	0.65	0.11	0.06	0.12	**0.05**
4	$CH_3 \leftarrow CH_3^-$	0.08	**0.00**	−0.07	−0.02	−0.07
5	$NH \leftarrow NH^-$	0.38	0.10	**0.02**	0.10	0.04
6	$NH_2 \leftarrow NH_2^-$	0.74	0.03	−0.06	**0.01**	−0.05
7	$O \leftarrow O^-$	1.46	0.20	**0.10**	0.19	0.14
8	$OH \leftarrow OH^-$	1.83	0.02	−0.08	**0.00**	−0.05
9	$F \leftarrow F^-$	3.40	0.15	**0.02**	0.11	0.07
10	$O_2 \leftarrow O_2^-$	0.44	−0.04	−0.10	**−0.02**	−0.07
11	$NO \leftarrow NO^-$	0.02	0.24	**0.21**	0.26	**0.21**
12	$CN \leftarrow CN^-$	3.82	−0.01	−0.06	**0.00**	−0.06
13	$Si \leftarrow Si^-$	1.38	0.08	0.05	0.08	**0.04**
14	$P \leftarrow P^-$	0.75	0.10	0.06	0.11	**0.04**
15	$S \leftarrow S^-$	2.08	0.06	**0.00**	0.06	**0.00**
16	$Cl \leftarrow Cl^-$	3.62	0.03	−0.04	**0.01**	−0.04
17	$SiH \leftarrow SiH^-$	1.28	0.10	0.06	0.09	**0.05**
18	$^1SiH_2 \leftarrow SiH_2^-$	1.12	0.15	0.12	0.15	**0.11**
19	$SiH_3 \leftarrow SiH_3^-$	1.44	**−0.03**	−0.09	−0.04	−0.09
20	$PH \leftarrow PH^-$	1.00	0.05	**−0.01**	0.04	**−0.01**
21	$PH_2 \leftarrow PH_2^-$	1.26	**−0.01**	−0.08	−0.03	−0.08
22	$SH \leftarrow SH^-$	2.31	**0.01**	−0.06	**−0.01**	−0.06
23	$PO \leftarrow PO^-$	1.09	0.09	**0.07**	0.10	0.06
24	$S_2 \leftarrow S_2^-$	1.66	−0.10	−0.13	**−0.08**	−0.14
25	$Cl_2 \leftarrow Cl_2^-$	2.39	0.24	0.26	0.30	0.25
	MAD	⋯	0.101	**0.091**	0.099	**0.091**

tory results for He_2, but significantly underbinds Ne_2 and Ar_2. B86PBE and xPBE reduce the overbinding tendency of PBE for He_2 and Ne_2 and give the best description of Ne_2.

Based on these results we expect that xPBE should lead to a good description of the London forces between electron pairs involving the first ten atoms of the periodic table, making it useful for the most common organic and biological systems.

It is well known that the long-range correlation is absent in the conventional density functionals.[54–57] Fundamental improvement on the functional is needed to describe correctly the physics of the long-range London-dispersion interactions.[58,59]

F. Bonding properties of water dimer

Hydrogen bonding plays a critical role in a wide range of chemical and biological phenomena. Thus water dimer, the prototypical hydrogen bonded system, has received much experimental and theoretical attention.[60–68] One difficulty in assessing the accuracy in the DFT methods is that the experimental determinations of R_e and D_e have been unreliable due to the floppy nature of the dimer. Microwave measurements lead to a vibrationally averaged O...O distance of $R_0 = 2.976$ Å, from which it was estimated that $R_e = 2.952$ Å.[64] The widely accepted experimental D_e of 5.44 ± 0.7 kcal/mol (Ref. 68) is indirect, being based on the interpretation of

TABLE X. Proton affinities (in kcal/mol) at 0 K for the eight systems of $G2$ (Refs. 7 and 29) and the deviations (theory-expt.) obtained from PBE, revPBE, B86PBE, and xPBE using aug-cc-pVTZ. $G2$ geometries (Refs. 27 and 28) are used in the DFT calculations. The best DFT results are in **boldface**.

No.	System	Expt.	PBE	revPBE	B86PBE	xPBE
1	$H_2 \leftarrow H_3^+$	100.8	−1.23	**−0.15**	−0.74	−0.75
2	$NH_3 \leftarrow NH_4^+$	202.5	−1.02	0.52	**−0.20**	−0.22
3	$H_2O \leftarrow H_3O^+$	165.1	−2.42	**−1.28**	−1.90	1.99
4	$C_2H_2 \leftarrow C_2H_3^+$	152.3	**−0.25**	2.52	1.38	1.24
5	$SiH_4 \leftarrow SiH_5^+$	154.0	−1.06	1.43	**0.53**	0.53
6	$PH_3 \leftarrow PH_4^+$	187.1	−3.98	**−1.70**	−2.51	2.53
7	$H_2S \leftarrow H_3S^+$	168.8	−1.61	**0.23**	−0.46	−0.42
8	$HCl \leftarrow H_2Cl^+$	133.6	**−0.02**	1.69	0.90	0.90
	MAD	⋯	1.450	1.190	1.077	**1.074**

TABLE XI. Bonding properties of He_2, Ne_2, and Ar_2 calculated by PBE, revPBE, B86PBE, and xPBE using the aug-cc-pVTZ($-f$) basis set. Bond energies are corrected for basis set superposition error (BSSE) effects. Bond lengths are in Å and bond energies are in kcal/mol. The best DFT results are in **boldface**.

	R(He-He)	ΔE(He-He)	R(Ne-Ne)	ΔE(Ne-Ne)	R(Ar-Ar)	ΔE(Ar-Ar)
PBE	2.752	0.074	**3.097**	0.111	**4.000**	**0.126**
revPBE	3.121	**0.028**	3.454	0.049	4.695	0.031
B86PBE	**2.864**	0.055	3.217	**0.082**	4.266	0.075
xPBE	2.847	0.057	3.197	**0.086**	4.250	0.078
Expt.[a]	2.970	0.022	3.091	0.084	3.757	0.285

[a]Reference 44.

measurements of the thermal conductivity of the water vapor. Indeed the most reliable values for the equilibrium geometry and dissociation energy of $(H_2O)_2$ are from CCSD(T) (full) coupled cluster calculations using both single and double substitutions from the Hartree-Fock determinant, and including triple excitations noniteratively (with basis sets extrapolated to infinity). This best *ab initio* calculation leads to $R_e(O...O) = 2.912 \pm 0.005$ Å and $D_e = 5.02 \pm 0.10$ kcal/mol.[62]

Table XII lists the calculated bonding properties of $(H_2O)_2$ from different DFT methods in the PBE family. We see that xPBE leads to R_e too long by 0.043 Å with a bond energy too weak by 0.56 kcal/mol. PBE leads to better results, with a bond too short by 0.023 Å and too strong by only 0.09 kcal/mol.

The elongation of the O-H bond in the donor water provides a third test of the quality of the description. The best *ab initio* estimate of $\Delta R_d(OH) = 0.007$ Å is from Bleiber and Sauer[63] using the fourth-order Møller-Plesset (MP4) method with the VTZ($2df$) basis on O and VTZ($2p$) on H PBE leads to $\Delta R_d(OH) = 0.011$ Å, a significant overestimate of this quantity, while xPBE leads to 0.009 Å.

Another parameter of interest is the frequency shift $\Delta \nu_d(OH)$ in the donor O-H stretching mode upon forming a hydrogen bond. In calculating this shift we use as the reference OH mode the arithmetic mean of the symmetric and the asymmetric harmonic stretching modes of the free monomer (since there is a strong coupling of these two modes for H_2O

monomer[63]). The experimental harmonic frequencies of water monomer and dimer lead to $\Delta \nu_d(OH) = -170$ cm^{-1}.[65–67] The best *ab initio* value obtained by Bleiber and Sauer at MP4/VTZ($2df,2p$) is -121 cm^{-1},[63] underestimating the frequency shift by 49 cm^{-1}. The DFT generally performs better with errors in $\Delta \nu_d(OH)$ of 47 (RBE) and 17 cm^{-1} (xPBE).

As seen from Table XII, it remains a challenge for a pure DFT method to give a good overall description of water dimer. While PBE gives the best predictions on $R_e(O...O)$ and D_e, PBE leads to clear overbinding, with concomitant overestimation of $\Delta R_d(OH)$ and $\Delta \nu_d(OH)$. On the other hand, revPBE gives the best predictions on $\Delta R_d(OH)$ and $\Delta \nu_d(OH)$, but revPBE shows clear underbinding with a too long $R_e(O...O)$ and a too small D_e. Values from xPBE are always close to the best numbers for all four properties, leading us to conclude that xPBE is the most balanced method in the PBE family for the description of hydrogen bonds.

V. CONCLUDING REMARKS

Development of improved approximations to the exchange-correlation functional is the key to the continued improvement in the success of Kohn-Sham density functional theory. A variety of exchange-correlation functionals have been developed, each with strengths and limits. We believe that the best strategy for developing improved approximations to the exact exchange-correlation functional within the GGA framework is to combine theory-based physical constraints with fitting a very limited set of parameters to selected experimental data. The physical constraints help to confine the functional forms; but the small gradient/high density regions and the large gradient/low density regions cannot be uniquely fixed by the physical constraints. But it is important to limit the number of empirical parameters in the functional (by making maximum use of physical concepts) so that systematic improvements of the functional can be achieved.

In line with this approach we started with the well-founded PBE functional[11] and extended it by optimizing the $(\mu,\kappa,\alpha,\beta)$ parameters against the experimental *atomic* data and the van der Waals interaction properties of Ne_2. (No other molecular information was used.) This xPBE functional significantly outperforms PBE in the prediction of the atomic data (exchange energies, correlation energies, and total energies for atoms from H to Ar) and the heats of formation (against the extended $G2$ sets), while maintaining the good performance of PBE for predicting geometry param-

TABLE XII. Bonding properties of water dimer. The DFT calculations used the aug-cc-pVTZ($-f$) basis set. The reference data and the best DFT results are in **boldface**.

	R_e(O...O)	ΔR_d(OH)[a]	$\Delta \nu_d$(OH)[b]	D_e
PBE	**2.899**	0.011	−217	**5.11**
revPBE	3.018	**0.007**	**−164**	3.58
B86PBE	2.957	0.010	−206	4.39
xPBE	2.955	0.009	−187	4.46
Best *ab initio*	**2.912±0.005**[c]	0.007[d]	−121[d]	**5.02±0.10**[c]
Expt.	2.952[e]	···	−170[f]	5.44±0.7[g]

[a]The enlongation of the O-H bond in the donor water.

[b]The frequency shift of the donor O-H stretching mode experienced upon forming a hydrogen bridge.

[c]Reference 62, CCSD(T)(full) IO275→∞ (IO275: interaction optimized basis set with 275 basis functions for H_2O dimer O—$7s5p5d3f2g1h$; H_d—$2s4p1d$, H—$2s3p$, BF—$3s3p2d1f$).

[d]Reference 63, MP4/VTZ($2df$) on O and VTZ($2p$) on H.

[e]Reference 64.

[f]References 65–67.

[g]Reference 68. Experimental D_e was estimated by adding the zero-point energy calculated at HF/4-21G level.

eters, ionization potentials, electron affinities, and proton affinities (against the extended $G2$ sets) and for describing van der Waals and hydrogen bond interactions.

Comparing to BLYP,[9,16] xPBE shows competitive quality in the predictions of the atomic data and the heats of formation of molecular systems. xPBE shows better quality in the predictions of ionization potentials, electron affinities, and proton affinities (against the extended $G2$ set). In particular, xPBE significantly outperforms BLYP in describing the van der Waals interactions.

As compared to PW91 (GGA II),[10,17] xPBE corrects, to a great extent, the overbinding tendency in the prediction of the heats of formation against the extended $G2$ sets, as well as in the description of the van der Waals interactions as represented by He_2 and Ne_2.

We also present here a detailed systematic validation of two other modified versions of PBE: revPBE (Refs. 11 and 12) and B86PBE.[11,16] Both functionals significantly improve upon PBE for predicting atomic data and the heats of formation (against the extended $G2$ set), but revPBE shows a clear tendency for underestimating the van der Waals and hydrogen bond interactions and is poorer than PBE for geometric predictions.

We conclude that xPBE provides a balanced description in covalent bonds as well as the van der Waals and hydrogen bond interactions. Thus xPBE should find applications in a wide range of important chemical and biological systems.

ACKNOWLEDGMENTS

[1] R. G. Parr and W. Yang, *Density Functional Theory of Atoms and Molecules* (Oxford University Press, New York, 1989).
[2] W. J. Hehre, L. Radom, P. V. R. Schleyer, and J. A. Pople, *Ab Initio Molecular Orbital Theory* (Wiley, New York, 1986).
[3] P. A. M. Dirac, Proc. Cambridge Philos. Soc. **26**, 376 (1930).
[4] J. C. Slater, *Quantum Theory of Molecules and Solids* (McGraw-Hill, New York, 1974), Vol. 4.
[5] S. H. Vosko, L. Wilk, and M. Nusair, Can. J. Phys. **58**, 1200 (1980).
[6] R. O. Jones and O. Gunnarsson, Rev. Mod. Phys. **61**, 689 (1989).
[7] D. C. Langreth and M. J. Mehl, Phys. Rev. B **28**, 1809 (1983).
[8] J. P. Perdew and Y. Wang, Phys. Rev. B **33**, 8800 (1986).
[9] A. D. Becke, Phys. Rev. A **38**, 3098 (1988).
[10] J. P. Perdew, in *Electronic Structure of Solids '91*, edited by P. Ziesche and H. Eschrig (Akademie, Berlin, 1991), p. 11.

[11] J. P. Perdew, K. Burke, and M. Ernzerhof, Phys. Rev. Lett. **77**, 3865 (1996).
[12] Y. Zhang and W. Yang, Phys. Rev. Lett. **80**, 890 (1998).
[13] B. Hammer, L. B. Hansen, and J. K. Norskov, Phys. Rev. **59**, 7413 (1999).
[14] C. Adamo and V. Barone, J. Chem. Phys. **116**, 5933 (2002).
[15] A. D. Becke, J. Chem. Phys. **84**, 4524 (1986).
[16] C. Lee, W. Yang, and R. G. Parr, Phys. Rev. B **37**, 785 (1988).
[17] J. P. Perdew and Y. Wang, Phys. Rev. B **45**, 13244 (1992).
[18] M. Filatov and W. Thiel, Mol. Phys. **91**, 847 (1997).
[19] P. M. W. Gill, Mol. Phys. **89**, 433 (1996).
[20] F. A. Hamprecht, A. J. Cohen, D. J. Tozer, and N. C. Handy, J. Chem. Phys. **109**, 6264 (1998).
[21] C. Adamo and V. Barone, J. Chem. Phys. **108**, 664 (1998).
[22] W.-M. Hoe, A. J. Cohen, and N. C. Handy, Chem. Phys. Lett. **341**, 319 (2001).
[23] E. H. Lieb and S. Oxford, Int. J. Quantum Chem. **19**, 427 (1981).
[24] M. Levy, Int. J. Quantum Chem. **S23**, 617 (1989).
[25] A. J. Cohen and N. C. Handy, Chem. Phys. Lett. **316**, 160 (2000).
[26] A. D. Becke, J. Chem. Phys. **98**, 5648 (1993).
[27] L. A. Curtiss, K. Raghavachari, G. W. Trucks, and J. A. Pople, J. Chem. Phys. **94**, 7221 (1991).
[28] L. A. Curtiss, K. Raghavachari, P. C. Redfern, and J. A. Pople, J. Chem. Phys. **106**, 1063 (1997).
[29] L. A. Curtiss, P. C. Redfern, K. Raghavachari, and J. A. Pople, J. Chem. Phys. **109**, 42 (1998).
[30] M. Rasolt and D. J. W. Geldart, Phys. Rev. B **34**, 1325 (1986).
[31] L. J. Sham, in *Computational Methods in Band Theory*, edited by P. Marcus, J. F. Janak, A. R. Williams (Plenum Press, New York, 1971).
[32] D. C. Langreth and J. P. Perdew, Phys. Rev. B **21**, 5469 (1980).
[33] E. K. U. Gross and R. M. Dreizler, Z. Phys. A **302**, 103 (1981).
[34] C. Lee and Z. Zhou, Phys. Rev. A **44**, 1536 (1991).
[35] L. Kleinman, Phys. Rev. B **30**, 2223 (1984).
[36] A. D. Becke, Int. J. Quantum Chem. **23**, 1915 (1983).
[37] S. K. Ghosh and R. G. Parr, Phys. Rev. A **34**, 785 (1986).
[38] T. Tsuneda, M. Kamiya, N. Morinaga, and K. Hirao, J. Chem. Phys. **114**, 6505 (2001).
[39] J. P. Perdew, K. Burke, and Y. Wang, Phys. Rev. B **54**, 16533 (1996).
[40] D. J. Lacks and R. G. Gordon, Phys. Rev. A **47**, 4681 (1993).
[41] E. Engel and S. H. Vosko, Phys. Rev. A **47**, 2800 (1993).
[42] S. J. Chakravorty and E. R. Davidson, J. Phys. Chem. **100**, 6167 (1996).
[43] J. F. Ogilvie and F. Y. H. Wang, J. Mol. Struct. **273**, 277 (1992).
[44] M. Levy and J. P. Perdew, Phys. Rev. A **32**, 2010 (1985).
[45] B. G. Johnson, P. M. W. Gill, and J. A. Pople, J. Chem. Phys. **98**, 5612 (1992).
[46] X. Xu and W. A. Goddard III, Proc. Natl. Acad. Sci. USA, **101**, 2673 (2004).
[47] J. P. Perdew, K. Burke, and M. Ernzerhof, Phys. Rev. Lett. **80**, 891 (1998).
[48] N. Rösch and S. B. Trickey, J. Chem. Phys. **106**, 8940 (1997).
[49] T. V. Mourik and R. J. Gdanitz, J. Chem. Phys. **116**, 9620 (2002).
[50] J. M. Galbraith and H. F. Schaefer, J. Chem. Phys. **105**, 862 (1996).
[51] J. M. Pérez-Jordá and A. D. Becke, Chem. Phys. Lett. **233**, 134 (1995).
[52] S. Kristyan and P. Pulay, Chem. Phys. Lett. **229**, 175 (1994).
[53] Y. Zhang, W. Pan, and W. Yang, J. Chem. Phys. **107**, 7921 (1997).
[54] D. C. Patton and M. R. Pederson, Phys. Rev. A **56**, R2495 (1997).
[55] T. A. Wesolowski, O. Parisel, Y. Ellinger, and J. Weber, J. Phys. Chem. A **101**, 7818 (1997).
[56] Y. Andersson, D. C. Langreth, and B. I. Lundqvist, Phys. Rev. Lett. **76**, 102 (1996).
[57] J. F. Dobson and B. D. Dinte, Chem. Phys. Lett. **76**, 1780 (1996).
[58] W. Kohn, Y. Meir, and D. E. Makarov, Phys. Rev. Lett. **80**, 4153 (1998).
[59] Q. Wu and W. Yang, J. Chem. Phys. **116**, 515 (2002).
[60] K. Kim and K. D. Jordan, J. Phys. Chem. **98**, 10089 (1994).
[61] D. A. Estrin, G. Daglieri, G. Corongiu, and E. Clementi, J. Phys. Chem. **100**, 8701 (1996).
[62] W. Klopper, J. G. C. M. van Duijneveldt-vande Rijdt, and F. B. van Duijneveldt, Phys. Chem. Chem. Phys. **2**, 227 (2000).
[63] A. Bleiber and J. Sauer, Chem. Phys. Lett. **238**, 243 (1995).
[64] J. A. Odutola and T. R. Dyke, J. Chem. Phys. **72**, 5062 (1980).
[65] W. S. Benedict, N. Gailan, and E. K. Plyler, J. Chem. Phys. **24**, 1139 (1956).
[66] L. Fredin, B. Nelander, and G. Ribbegard, J. Chem. Phys. **66**, 498 (1977).
[67] B. Nelander, J. Chem. Phys. **69**, 3870 (1978).
[68] L. A. Curtiss, D. J. Frurip, and M. Blander, J. Chem. Phys. **71**, 2703 (1979).